

Spring 5-3-2022

Segmentation of DNA Lesions in Irradiated Mouse Brain Sections

Nicholas Cirone

Northern Illinois University, Z1904360@students.niu.edu

Follow this and additional works at: <https://huskiecommons.lib.niu.edu/studentengagement-honorscapstones>



Part of the [Cell and Developmental Biology Commons](#)

Recommended Citation

Cirone, Nicholas, "Segmentation of DNA Lesions in Irradiated Mouse Brain Sections" (2022). *Honors Capstones*. 1411.

<https://huskiecommons.lib.niu.edu/studentengagement-honorscapstones/1411>

This Article is brought to you for free and open access by the Undergraduate Research & Artistry at Huskie Commons. It has been accepted for inclusion in Honors Capstones by an authorized administrator of Huskie Commons. For more information, please contact jschumacher@niu.edu.

NORTHERN ILLINOIS UNIVERSITY

Segmentation of DNA Lesions in Irradiated Mouse Brain Sections

A Capstone Submitted to the

University Honors Program

In Partial Fulfillment of the

Requirements of the Baccalaureate Degree

With Honors

Department Of

Biological Sciences

By

Nicholas Cirone

DeKalb, Illinois

May 2022

University Honors Program
Capstone Faculty Approval Page

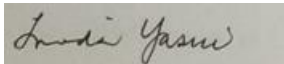
Capstone Title (print or type)

Segmentation of DNA Lesions in Irradiated Mouse Brain Sections

Student Name (print or type) **Nicholas Cirone**

Faculty Supervisor (print or type) **Linda Yasui**

Faculty Approval Signature



Department of (print or type) **Biological Sciences**

Date of Approval (print or type) May 3rd, 2022

Date and Venue of Presentation **Phi Sigma Symposium (April 20 – April 22, 2022)**

Check if any of the following apply, and please tell us where and how it was published:

Capstone has been published (Journal/Outlet):

Capstone has been submitted for publication (Journal/Outlet):

Completed Honors Capstone projects may be used for student reference purposes, both electronically and in the Honors Capstone Library (CLB 110).

If you would like to opt out and not have this student's completed capstone used for reference purposes, please initial here: _____ (Faculty Supervisor)

Abstract

The impacts of microscopy image analysis have resulted in better visualization of foci (spots) in cell nuclei. However, manual analysis of microscopy images is challenging regarding subjectivity in structure counting and identification. Recent computer algorithms have enabled cellular analysis through automatic segmentation that uses computational edges in digital images. In this project, the automatic segmentation workflow in the Zeiss Zen Blue 3.3 software was adapted to more closely reflect visualized foci in a cell. The foci represent DNA double strand breaks. The Zeiss LSM 900 microscope was used to collect maximal intensity projection images of γ H2AX foci and super-resolution z-stacks ($z = 1 \mu\text{m}$). The Zeiss Zen Blue 3.3 software was used to automatically score γ H2AX foci using global thresholding and background subtraction segmentation. After single U87 cell segmentation analysis, 8 Gy irradiated male and female mouse brain sections were automatically scored using the background subtraction method. Manual scoring of cell nuclei in mouse brain sections was used to calculate foci density (foci per cell) in male and female sections. Increased γ H2AX foci counts were observed in the irradiated male and female brain sections, which indicates the persistence of DNA lesions past normal DNA repair times. Irradiated male mice showed higher foci count and foci density compared to female mice, supporting established literature of increased male radiosensitivity. Automatic segmentation has the potential to provide an accurate and time-efficient method for foci scoring with further implementation to improve understanding of radiation-induced DNA damage for bettering therapeutic approaches toward males and females.

Introduction

Microscopy image analysis is an important method for understanding biological structures and functions. The development of powerful computers and software has allowed the combination of microscopy imaging with 3D modeling, maximal intensity projections, and automatic segmentation. In this experiment, super-resolution fluorescence microscopy was used to investigate and automatically segment DNA lesions in U87 glioblastoma cells and mouse brain sections. Segmentation is the process of partitioning an image into multiple components that are associated with a unique pixel range¹. Specifically, the segmentation process involves the labeling of pixels from which pixels with the same label also share similar characteristics¹. The goal of using segmentation was to process super-resolution images to isolate γ H2AX foci (DNA lesions) from non-related structures. Typically, segmented components are objects, curves, lines, or defined boundaries. Regional pixels are grouped based on similar characteristics of intensity, color, and texture, while adjacent pixels generally have significant deviation of characteristics². As a result, the analyzed image is separated into sets of segments or sets of contours. The applications of segmentation are widespread in medical imaging, object detection, and can be applied to scoring/counting structures³.

The development of microscopy software has allowed segmentation to become more time-efficient and accurate through automated processes^{1,2}. Automatic segmentation relies on user-set thresholds for the software to automatically separate objects based on intensities, sizes, color, and smoothness^{3,4}. In this project, Airyscan super-resolution images were used for applying automatic segmentation. Zeiss Efficient Navigation (Zen) Blue⁵ operates as a universal interface for balancing flexibility and simplicity for microscopy use⁵. The software consists of 'Locate', 'Acquisition', 'Processing', and 'Analysis' modules that provide a workflow starting

from image collection to image analysis and segmentation^{4,5}. The ‘Analysis’ module contains parameters, methods, and tools for image deconstruction, profiling, and automatic segmentation⁴. The Zen Blue automatic segmentation process follows a 7-step ‘Image Analysis Wizard’ that combines user-input with automated detection and results. In this experiment, segmented images were based on maximal intensity projection (MIP), which transforms 3D data (z-stacks) into a 2D image². MIP images of irradiated U87 cells and mouse brain sections were used to visualize DNA lesions.

The robust Zen Blue⁵ software was used to automatically segment the DNA double-strand break (DSB) biomarker, γ H2AX, in single cells and mouse brain sections. The γ H2AX biomarker is visible in the cell nucleus as fluorescent green foci. The foci represent an area of phosphorylation of serine 139 on histone H2AX, which is a crucial step in DNA double strand break sensing^{6,7}. Exposure to ionizing radiation, such as Cs-137 γ rays, can induce DSBs with foci formation and size indicating mechanisms and the extent of DSBs. Moreover, the determination of DSB repair through homologous recombination (HRR), nonhomologous end-joining (NHEJ), or other mechanisms can indicate repair processes to target for diagnosis and therapy⁶. The persistence of foci past normal DSB repair times can indicate continued DNA damage response through reactive oxygen species, altered chromatin structure, and/or inflammation responses⁸. Increased radiosensitivity of males compared to females can correspond with increased foci counts and persistence. The automatic segmentation process starting from single U87 cells to mouse brain sections was examined for γ H2AX foci and radiation-induced effects to better therapeutic approaches towards males and females.

Materials and Methods

U87 Cell Culture and Staining

The human glioblastoma cell line, U87, was grown in DMEM:F12 (1:1) 10% fetal bovine serum supplement with penicillin and streptomycin. The cells were irradiated with 2 Gy of Cs-137 decay to induce DNA damage. After irradiation, cells were stained with the primary anti-phospho-H2AX antibody followed by staining with a secondary FITC-IgG antibody stain for green fluorescence of γ H2AX foci. DAPI blue counter stain was applied to identify nuclei.

Mouse Brain Sections⁹

Ten female and ten male BALBc mice were maintained on a 12:12 light/dark cycle. Female and male mice were whole-body irradiated with 8 Gy of Cs-137 γ rays (n = 5) or were assigned to sham (n = 5). After irradiation, mouse health and weight were monitored weekly for radiation-induced effects. Fifteen days post-irradiation, mouse brains were overnight fixed (4°C in 4% paraformaldehyde) then cryoprotected (30% sucrose in PBS, pH 7.4). Brains were cryo-sectioned with coronal sectioning at 40 μ m thickness. See “The DNA damage response in whole mouse brains exposed to 8 Gy γ rays”⁹ poster for experimental design and methods.

Immunohistochemistry

Antigen retrieval was applied (90°C in 10 mM sodium citrate, pH 6.0, for three minutes). Phosphate-buffered saline (0.2% Tween-20, 5% normal goat serum, pH 7.4) was used to dilute antibodies. The brain sections were incubated with primary antibodies at 4°C overnight. Secondary antibody incubation proceeded at room temperature for one hour. The sections were mounted on gelatin-subbed slides followed by cover-slipping with IBIDI mounting medium containing DAPI.

Image Collection

The Zeiss LSM 900 Microscope (Figure 1) was used to collect Airyscan super-resolution images and z-stacks ($z = 1 \mu\text{m}$). U87 cell images were collected using the 63x objective. Mouse brain images were sampled in the hippocampal and cortical areas using either the 20x or 63x objectives. In the Zen Blue software, an Airyscan line acquisition method was used to automatically separate channels based on fluorescent dyes used in the experiment. γH2AX foci were visualized using a green channel that detected the secondary FITC-IgG staining. Nuclei were isolated using a blue channel that detected DAPI staining. ‘Master Gain’ and ‘Laser Power’ settings for FITC-IgG and DAPI channels were adjusted to ensure the entire dynamic range of the green and blue channels were sampled by ensuring the signal from the green and blue channels full covered the signal histogram. Maximal intensity projection (MIP) images were collected by orthogonal projection of z-stacks followed by conversion of 3D (z-stack) data to single 2D images. MIP images were generated for U87 cells and for mouse brain sections to be used for segmentation analysis.



Figure 1. Zeiss LSM 900 Microscope and set-up. The confocal laser scanning microscope was used for Airyscan 2 super-resolution imaging. The Zen Blue⁵ software was used to acquire z-stacks and generate MIP images of U87 cells and mouse brain sections for automatic segmentation.

Foci Segmentation Overview

The Zen Blue software was used for automatic segmentation with a seven-step workflow (Figure 2). The class set-up was assigned to the green, fluorescent FITC channel to detect γ H2AX foci. For single cell segmentation, the frame encompassed the entire cell. For mouse brain section segmentation, cells were cropped to fill the field of view. Single cell automatic scoring was accomplished using the global thresholding and segment by background subtraction methods. Automatic scoring of foci in mouse brain sections was done using segment by background subtraction. Subsequent region filters and interaction segmentation methods were not applied. The 'Count' setting was applied in the 'Features' step to automatically list the number of foci. After automatic segmentation of foci, manual scoring of nuclei in mouse brain sections was accomplished using z-stacks and MIP images. Foci densities (foci per cell) and foci counts were examined in male and female mouse hippocampal and cortical sections.



Figure 2. 7-step Image Analysis Wizard workflow. The Zen Blue software was used to automatically segment γ H2AX foci. Fluorescent green foci were assigned the primary class followed by image framing and automatic segmentation using global thresholding and background subtraction.

Zen Blue⁵ Global Thresholding Method

Automatic segmentation using global thresholding required additional sharpening parameters to identify γ H2AX foci. The ‘delineate’ sharpening parameter identified foci by tracing boundary foci pixels with the highest intensities⁴. Delineate sharpening was selected with a threshold value of 150 and a size value of 5 to improve the pixel boundaries of foci. The Otsu Threshold (Light Regions) method was used to target foci pixels over background pixels. Further identification of foci used ‘Open Binary’ with a count of 2 and ‘Morphology Separate’ with a count of 5. Binary and morphology parameters reduced the clustering of multiple foci into a single focus.

Zen Blue⁵ Segment by Background Subtraction Method

Automatic segmentation using background subtraction used the median smoothing parameter with a size of 3 to reduce blurriness of the foci. The degree of background subtraction was modified using ‘Rolling Ball Subtract BG’ with a radius of 25. Delineate sharpening was used with a threshold of 140 and a size of 5. The Otsu Threshold (Light Regions) method was used to target foci pixels over background pixels. Further identification of foci used ‘Open Binary’ with a count of 3 and ‘Morphology Separate’ with a count of 6.

Results

Single Cell Automatic Segmentation

The global thresholding and segment by background subtraction methods were used to perform automatic segmentation on single cells. Global thresholding (Figure 3, #1) targeted the pixels with the highest intensities of a specific class. In this experiment, the fluorescent green γ H2AX foci class was targeted, which resulted in foci pixels being selected and non-foci pixels being excluded. Global thresholding showed optimal results when background interference or noise was minimal. The second segmentation method, background subtraction (Figure 3, #2), separated foreground pixels from background pixels to isolate γ H2AX foci. Foreground pixels generally had a higher intensity compared to the background pixels, which had low deviation. Background fluorescent green pixels were excluded from foci fluorescent green pixels. The background subtraction segmentation method showed optimal results when background intensities were low-deviating and different from foci intensities of the same class. Both segmentation methods were modified using smoothing and sharpening processes to further isolate foci from the blue DAPI nucleus stain. Foci diameters were restricted to the range of 0.5 μm – 1.5 μm to mitigate under/overcounting.

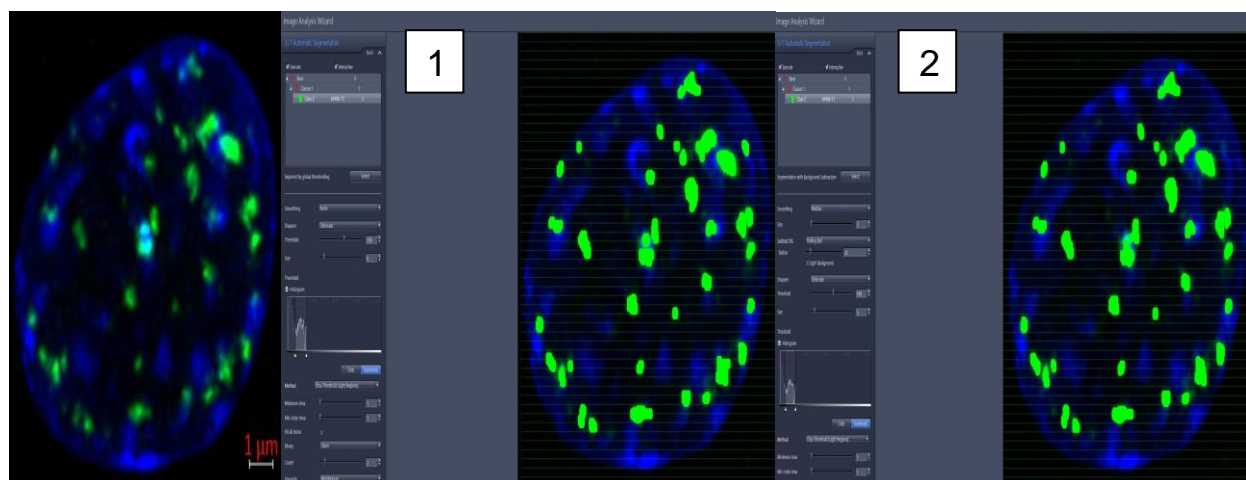


Figure 3. U87 glioblastoma cell segmentation methods. Global thresholding (1) and background subtraction (2) were compared using a representative image of a U87 cell exposed to 2 Gy that was acquired using Airyscan and processed as a MIP image (leftmost picture). Additional smoothing and sharpening processes were modified to isolate green fluorescent foci pixels from the DAPI blue background.

Mouse Brain Sections Automatic Segmentation

Super-resolution MIP images of female and male mouse brain sections were collected from hippocampal and cortical areas. Unirradiated mouse brain sections (Figure 4) showed the residual persistence of γ H2AX foci in cortical and hippocampal areas. Irradiated mouse brain sections (Figure 5) showed increased foci persistence, size, and counts in hippocampal and cortical areas compared to unirradiated sections. The FITC-IgG marker showed increased intensity for irradiated samples. Female brain sections showed lower foci counts compared to male sections. For both unirradiated and irradiated sections, FITC background interference was observed that interfered with foci identification. Automatic segmentation was applied to male and female brain sections to further identify foci from background noise and non-related structures. The background subtraction method established from U87 cell segmentation was used to reduce background noise. The global thresholding method did not discriminate the background noise from the foci to obtain reasonable counts.

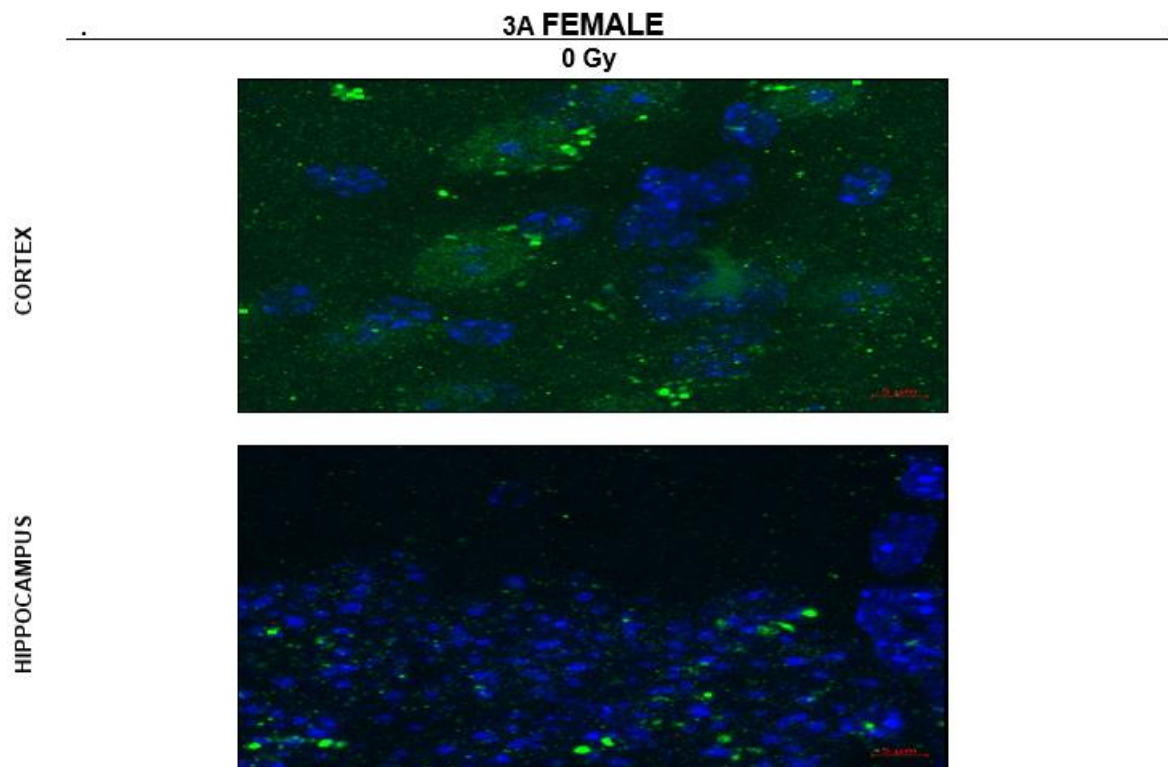


Figure 4. Unirradiated mouse brain sections. Super-resolution MIP images of a representative unirradiated mouse brain, 3A, were examined for foci scoring, size, and persistence. Foci persistence may indicate DNA damage in response to ROS and altered chromatin structures. FITC (green) background staining was more intense in cortical sections than hippocampal sections. Micron marker = 5 μm .

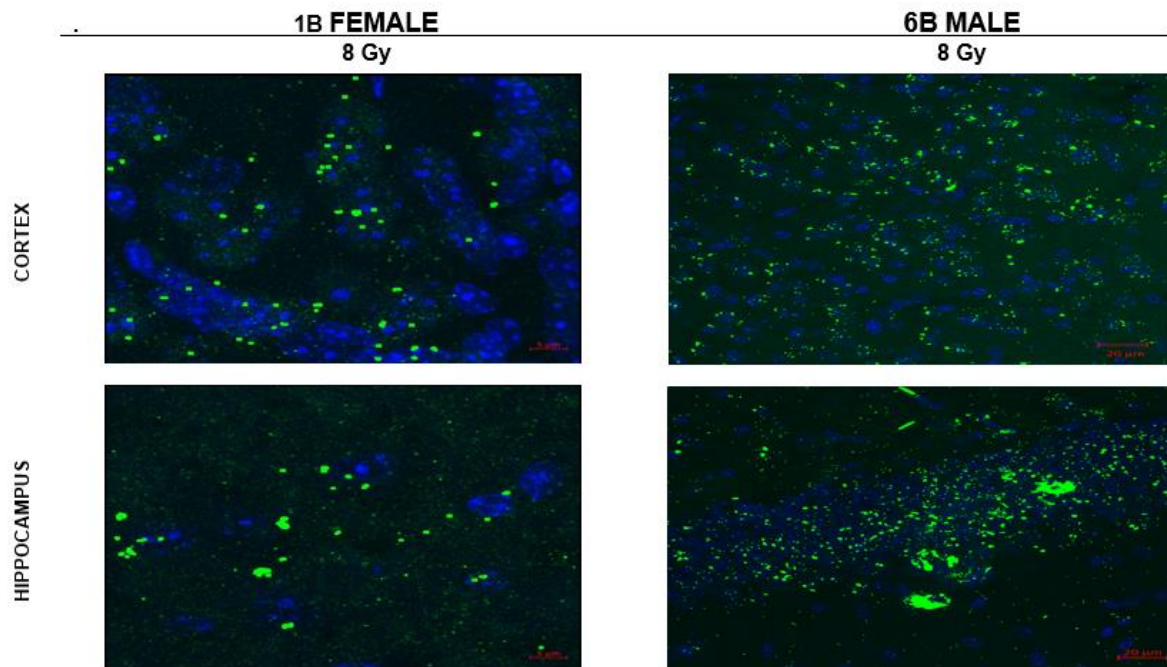


Figure 5. Irradiated mouse brain sections. Super-resolution MIP images of representative irradiated mouse brain sections, 1B and 6B, were examined for foci scoring, size, and persistence. Foci were found to be larger in size and in numbers than in unirradiated mice. Male sections showed increased foci persistence and counts compared to female sections. 1B female images micron marker = 5 μm . 6B male images micron marker = 20 μm .

Mouse Brain Foci and Nuclei Scoring

The background subtraction method for automatic scoring of foci in mouse brain sections returned higher foci counts in the irradiated mouse brain sections, 1B and 6B (Figure 6).

Hippocampal sections generally contained more cells and foci than cortical sections. The collection of data using 20x and 63x magnifications was used to empirically determine which field of view provided enough cells for statistical purposes. As a result, male brain sections contained a field of view with a larger cell count and a larger foci count. Subsequent manual counting of nuclei was accomplished by the scoring DAPI (blue) stained nuclei to examine cellular counts in brain sections and the average foci density. Manual nuclei scoring for the females was done using the same MIP images from foci scoring. However, nuclei scoring for

males required counting through multiple planes of z-stacks acquired during Airyscan imaging. The collected counts (Figure 7) for male cortical and hippocampal sections had lower confidence due to nuclei crowding and difficulty in discriminating separate nuclei.

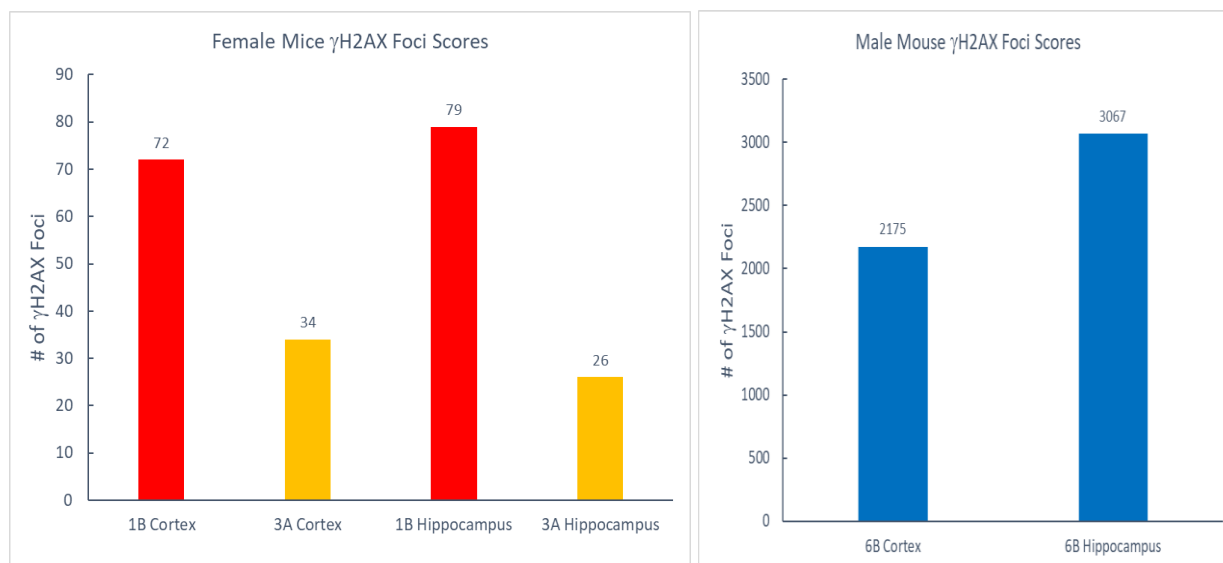


Figure 6. Automatic γ H2AX scoring of mouse brain sections. Female mouse scores (1B and 3A) were collected from super-resolution MIP images collected using a 63x objective. Male mouse scores (6B) were collected from super-resolution MIP images collected using a 20x objective.

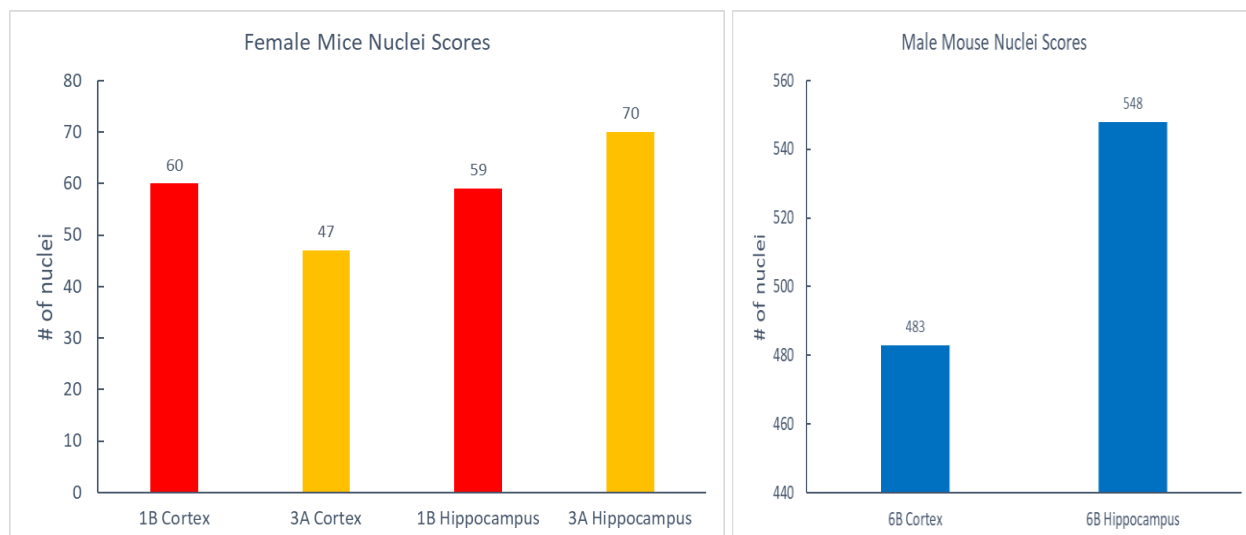


Figure 7. Manual nuclei scoring of mouse brain sections. The nuclei of male and female mouse brain sections (1B and 3A) were scored using the blue DAPI stain for identification. Female mouse scores were collected from super-resolution MIP images collected using a 63 objective. Male mouse scores (6B) were collected from super-resolution z-stack analysis collected using a 20x objective.

Mouse Brain Foci Densities and Persistence

The foci densities (foci per cell) of mouse brain sections were calculated by dividing foci counts (Figure 6) by manual nuclei counts (Figure 7) to evaluate foci persistence after a 15-day interval between irradiation and collection. Male cortical and hippocampal sections showed increased foci densities compared to female sections (Figure 8). In both males and females, hippocampal sections were found to have higher foci densities than cortical sections. The persistence of DNA damage in both males and females after 15 days (past normal DNA repair time) indicates possible stress responses and endogenous damage through ROS, altered chromatin structure, and inflammatory responses.

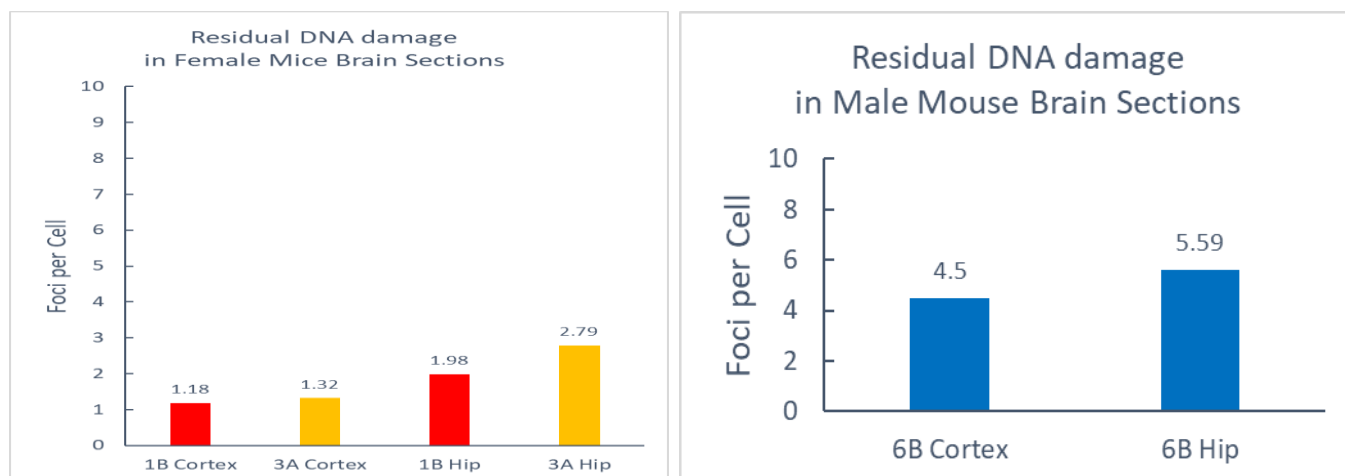


Figure 8. Foci per cell in Male and Female Brain Sections. The foci density (foci per cell) for mouse brain sections was calculated by dividing automatic foci scores (Figure 6) by manual nuclei scores (Figure 7). Foci densities in male sections were found to be higher than in female sections. In both males and females, hippocampal sections showed a higher foci density than cortical sections.

Discussion

The automatic segmentation of γ H2AX foci has the potential to be used for an accurate and time-efficient scoring method. Segmentation using global thresholding is most effective when background interference is minimal by increasing the signal-to-noise ratio. Segmentation by background subtraction can provide a reasonable scoring method when background interference is noticeable. Nevertheless, the minimization of background noise through modifying staining procedures provides optimal and unmodified images for accurate segmentation. Further segmentation modification using sharpening and smoothing processes can better discriminate foci pixels from the background. However, smoothing/sharpening can lead to de-selection that leaves out data, which may translate into miscounting or misidentification. Implementation of automatic segmentation on repeat trials can provide information regarding limitations of automatic scoring. Automatic segmentation can be expanded to analyze nuclei counts and be compared with manual counts for accuracy and deviation.

The automatic scoring of foci showed a higher γ H2AX count in irradiated mouse sections, which indicated residual DNA damage. We speculate that the persistence of γ H2AX foci in males and females past normal repair times indicates DNA damage caused by altered chromatin and/or reactive oxidative species. Subsequent manual scoring of nuclei and determination of foci densities showed an increased foci density in male mice compared to females. The increased foci counts found in males supports established literature of males being more radiosensitive than females¹⁰. Higher foci densities in male and female hippocampal sections compared to cortical sections may indicate persistent DNA damage stress responses in relation to location and extracellular environmental factors. Further optimization and implementation of automatic segmentation can improve understanding of the extent and location of radiation-induced DNA damage for bettering diagnosis and therapy for females and males.

Acknowledgements

I thank Dr. Linda Yasui, my faculty mentor/advisor, for providing expertise, support, and training. I also thank Julia Lentz, Matthew Ramlow, Ericka Schaeffer, and Dr. Doug Wallace for helping with experimental methods and data collection. I gratefully acknowledge the NIU Student Engagement Fund (SEF) for funding for purchasing commodities. I also gratefully acknowledge the National Science Foundation, Major Research Instrumentation Program (Award #2018748) for funding of the Zeiss LSM 900 microscope.

References

1. Cimini, B., Carpenter, A., Eliceiri, K., Li, B., Lucas, A., Ryder, P. (2021, February 18). Open-source deep-learning software for bioimage segmentation. *Molecular Biology of the Cell*, Vol. 32, No.9. doi:10.1091/mbc.E20-10-0660.
2. Belevich I, Joensuu M, Kumar D, Vihinen H, Jokitalo E (2016) Microscopy Image Browser: A Platform for Segmentation and Analysis of Multidimensional Datasets. *PLoS Biol* 14(1): e1002340. doi:10.1371/journal.pbio.1002340
3. Gargi V, Pednekar, Jayaram K, Udupa, David J, McLaughlin, Xingyu Wu, Yubing Tong, Charles B. Simone II, Joseph Camaratta, and Drew A. Torigian "Image quality and segmentation", Proc. SPIE 10576, Medical Imaging 2018: Image-Guided Procedures, Robotic Interventions, and Modeling, 105762N (13 March 2018); doi:/10.1117/12.2293622
4. Zeiss Zen. (n.d.). *A Beginner's Guide to Automated Image Analysis in ZEN Blue*. Retrieved from <https://www.zeiss.com/content/dam/Microscopy/us/download/pdf/zen-software-education-center/a-beginners-guide-to-image-analysis-in-zen-blue.pdf>
5. Zeiss. (2020). *Zen Blue* (Version 3.3). Munich, Germany: Carl Zeiss Microscopy GmbH
6. Rogakou, EP, Pilch DR, Orr AH, Ivanova VS, * Bonner WM. (1998, March 6). DNA double-stranded breaks induce histone H2AX phosphorylation on serine 139. *The Journal of Biological Chemistry*, 273(1), 5858-68. Doi:10.1074/jbc.273.10.5858.
7. D'Abrantes, S., Gratton, S., Reynolds, P., Kriechbaumer, V., McKenna, J., Barnard, S., Clarke, D. T., & Botchway, S. W. (2017, October 20). Super-resolution nanoscopy imaging applied to DNA double-strand breaks. *BioOne Complete*, 189(10), 19-31. doi:10.1667/RR14594.1

8. Acharya, M. M., Christie, L. A., Lan, M. L., Donovan, P. J., Cotman, C. W., Fike, J. R., & Limoli, C. L. (2009). Rescue of radiation-induced cognitive impairment through cranial transplantation of human embryonic stem cells. *Proceedings of the National Academy of Sciences*, *106*(45), 19150-19155. doi:10.1073/pnas.0909293106
9. Cirone, N., Lentz, J., Ramlow, M., Schaeffer, E., Wallace, D., Yasui, L. (2022, April). The DNA damage response in whole mouse brains exposed to 8 Gy γ rays. *Northern Illinois University*, Departments of Biological Sciences and Psychology.
10. El-Nachef, L., Al-Choboq, J., Restier-Verlet, J., Granzotto, A., Berthel, E., Sonzogni, L., Ferlazzo, M. L., Bouchet, A., Leblond, P., Combemale, P., Pinson, S., Bourguignon, M., & Foray, N. (2021, July 2). Human radiosensitivity and radiosusceptibility: What are the differences? *International Journal of Molecular Sciences*, *2021*, 22,7158.
Doi:10.3390/ijms22137158.